CHAPTER IV

RESULTS AND DISCUSSION

The NR composites reinforced by silica that was generated *in situ* were subjected to various analyses. The conversion of TEOS to silica, physical appearance of the composites, influences of the silica on mechanical properties, and a comparison to composites filled with silica powder are all covered in this chapter. Moreover, a statistical analysis, called 'Factorial Design', was used to study the influence of silica on the mechanical properties of the composites in a more efficient way.

4.1 Conversion of TEOS to Silica

TEOS was added with stirring directly into concentrated NR latex. The mixture was then baked and dried at 50°C. The silica content in the NR composite was determined prior to further sulfur curing. Data are shown in Table 4.1.

The amount of silica in the composites increases with increasing the amount of TEOS added to the latex. In all cases, the conversion from TEOS to silica (SiO_2) is 89-97% by mole, indicating that nearly all TEOS has turned into silica during the sol-gel process.

Table 4.1 The silica content and %conversion of TEOS to silica of the sol-gel process in NR

Sample	TEOS (phr)	Residue ash at 850 °C (%)	Silica content (%)	%Conversion from TEOS to silica
NRT 0	0	0.17 ± 0.01	0	0
NRT 10	10	2.82 ± 0.26	2.73 ± 0.26	94.63
NRT 20	20	5.04 ± 0.09	5.27 ± 0.16	91.48
NRT 30	30	7.22 ± 0.19	7.75 ± 0.19	89.67
NRT 40	40	9.53 ± 0.08	10.49 ± 0.08	91.05
NRT 50	50	12.44 ± 0.83	13.98 ± 0.83	97.10
NRT 60	60	14.12 ± 0.29	16.20 ± 0.29	93.77
NRT 70	70	16.30 ± 0.15	19.23 ± 0.15	95.40

4.2 Physical Appearance of the NR-Silica Composites

4.2.1 General Observation

TEOS is immiscible with water, but natural emulsifier present in the latex aids the mixing. When adding a small amount of TEOS, the mixture remains homogeneous and becomes more viscous when increasing TEOS content. But when the TEOS amount is larger than 70 phr, the mixture is so viscous that a homogeneous mixture can not be obtained.

Silica contents in the NR-silica composites are listed in Table 4.2.

Table 4.2 Composition of NR-silica composites of *in situ* and mechanically mixed silica

Silica generated *in situ*		Mechanically mixed silica	
Sample code	SiO_2 (%)	Sample code	SiO_2 (%)
I 2	2.73	M 2	2.70
I 5	5.14	M 5	5.10
I 7	7.61	M 7	7.60
I 10	10.34	M 10	10.30
I 13	13.98	M 13	13.90
I 16	16.20	M 16	16.20
I 19	19.23	M 19	19.20

Appearances of some composites listed in Table 4.2 are shown in Fig. 4.1. The composites become more opaque with increasing silica contents. One key observation made is that when the composite containing mechanically mixed silica is scratched, some silica powder in fact falls off. This does not occur with the composite containing *in situ* silica. *In situ* silica is indicated by I and mechanical silica is coded as M.
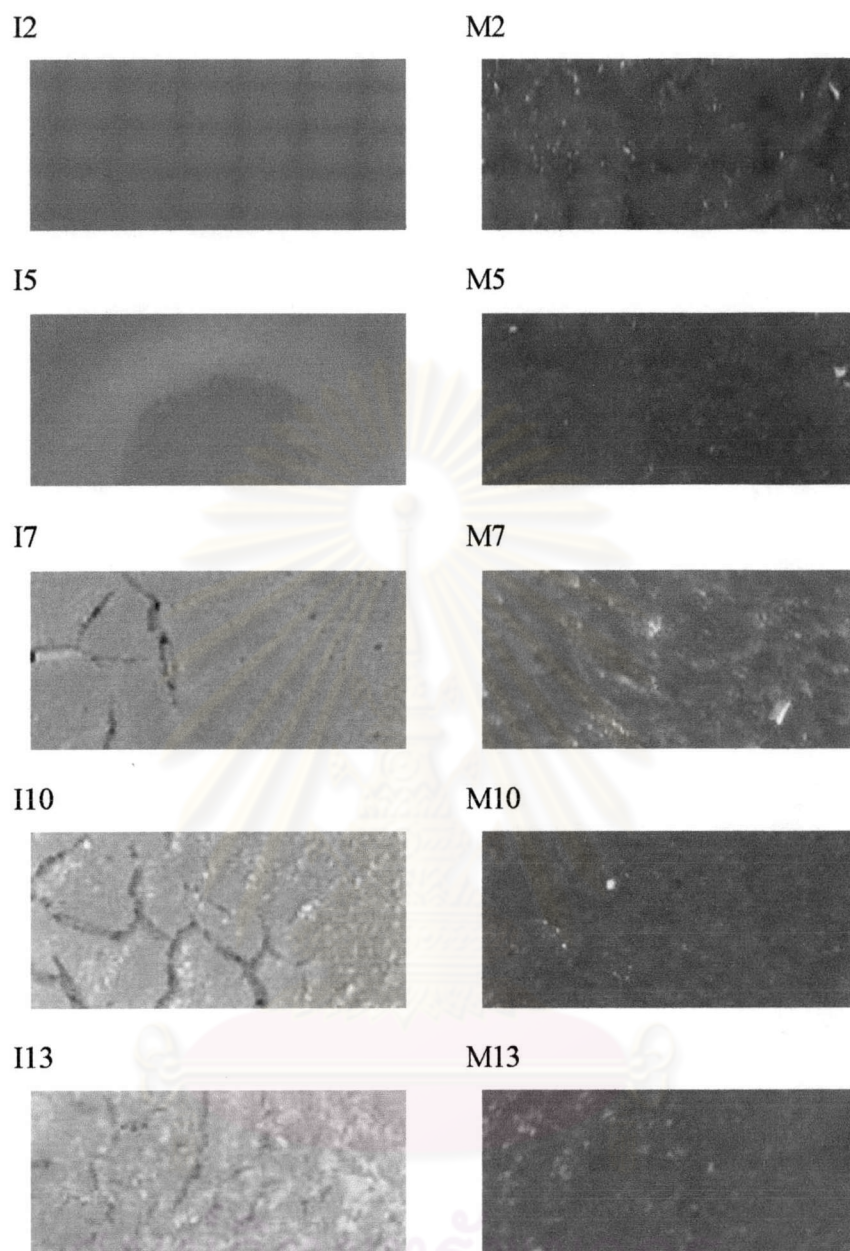
I2

M2

I5

M5

I7

M7

I10

M10

I13

M13

Figure 4.1 Photographs of NR composites filled with *in situ* silica (I) and mechanically mixed silica (M)

4.2.2 Morphology and Distribution of Silica in the Composite

The fracture surfaces of the composites listed in Table 4.2 were analyzed by using SEM (Fig. 4.2). White spots represent the silica particles and black area is the rubber matrix. The silica particles are evenly dispersed in the NR matrix. By comparing

the size of white spots on the micrographs, it is not clear whether the particle size increases with the amount of TEOS or not. TEM would be a better equipment to determine the particle size in the range of sub-micron. Unfortunately, analysis of TEM was not performed, due to the cryogenic sample preparation equipment was unoperational at the time of this study.
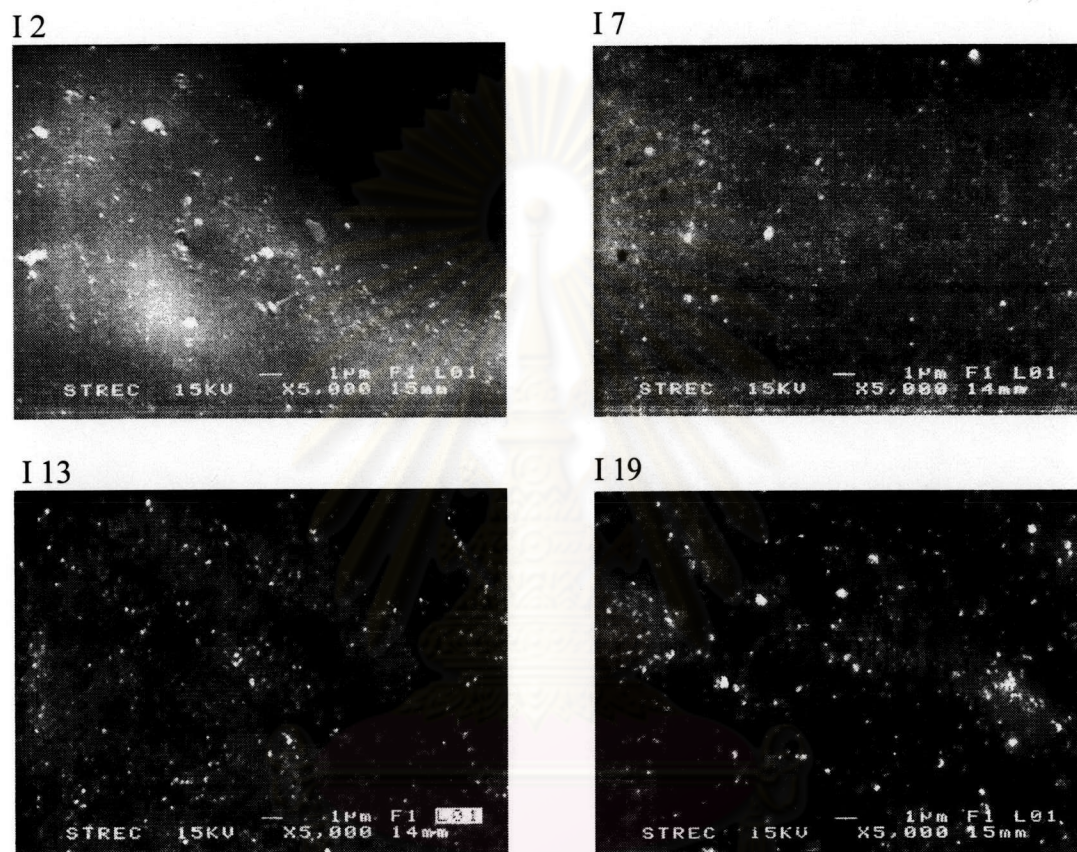
I 2

I 7

I 13

I 19

Figure 4.2 SEM micrographs of NR-silica composites filled with *in situ* silica (I)

4.2.3 The Size of Silica Particle in the Composites

Since SEM is not an effective method to determine the size of particle in the sub-micron range, TEM is used to analyze a sample of *in situ* silica-NR composite. Practically a cryogenic slicing machine is needed to cut out a thin rubber specimen. Unfortunately the machine was unoperational in Thailand, the rubber sample was therefore hardened by embedding the composite in polystyrene, then sliced to obtain a thin specimen for the TEM. It should be noted here that, since the composite was swollen in styrene, silica tended to disperse differently from the original state. Therefore dispersion of silica in the NR matrix cannot be determined.

Two TEM photographs of the composite having 10% silica (I10) are shown in Fig. 4.3. The silica particles aggregate to form clusters having various shapes and sizes. Single silica particle was measured on the picture using a ruler. An average diameter, out of five different silica particles, is 44.4 ± 0.1 nm.
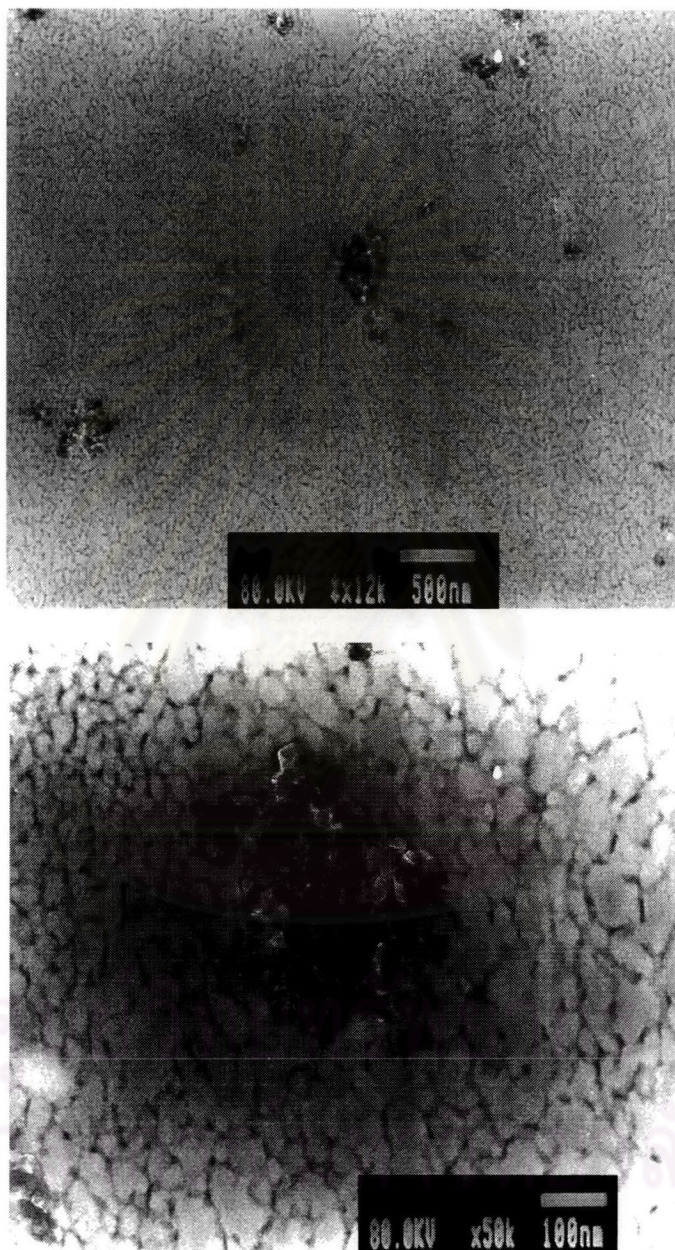

Figure 4.3 TEM images of NR-silica composite with 10 % *in situ* silica (I 10)

4.3   Experimental Design for Study Factors that Influence Mechanical Properties of NR-Silica Composite

The factorial design at two-level was carried out in order to study the factor thought to influence the mechanical properties such as tensile modulus, tensile strength, and tear strength. The three factors (k= 3) that were focused here are TEOS content (T), added ammonia (N), and gelation time (G). Each factor is present at two levels- high and low. The 2^3 factorial design with two replicates is used. A table of + and - signs for the 2^3 factorial design and the average response data are shown in Table 4.3. Raw data of each of the two replicates are shown in Appendix A.

Table 4.3 The sign of each factor and averaged response data from 2 replicate experiments

| Experiment | Factors | | | Silica content (%) | Modulus 300% elongation (MPa) | Tensile strength (MPa) | Tear strength (N/mm) |
	TEOS (T)	Added NH$_3$ (N)	Gelation time (G)				
ED 1	-	-	-	2.69 ± 0.23	1.87 ± 0.137	15.87 ± 1.28	33.57 ± 1.54
ED 2	-	-	+	2.82 ± 0.12	2.02 ± 0.192	16.22 ± 2.40	32.29 ± 1.49
ED 3	-	+	-	2.68 ± 0.08	2.09 ± 0.188	17.76 ± 2.76	32.59 ± 1.37
ED 4	+	-	-	13.00 ± 0.05	2.61 ± 0.344	23.48 ± 3.08	36.44 ± 1.63
ED 5	+	+	+	13.17 ± 0.25	2.96 ± 0.391	24.90 ± 1.42	37.81 ± 1.70
ED 6	+	+	-	13.29 ± 0.38	2.70 ± 0.227	22.07 ± 1.71	37.98 ± 1.95
ED 7	+	-	+	13.51 ± 0.67	2.80 ± 0.278	24.63 ± 1.35	40.95 ± 1.79
ED 8	-	+	+	2.54 ± 0.08	2.38 ± 0.270	18.80 ± 2.31	34.20 ± 1.96

TEOS: + (50 phr), - (10 phr); added NH$_3$: + (2.5 %), - (0 %); gelation time: + (10 days), - (5 days)

In order to conclude which effects influence the mechanical properties of the composites, comparison of the estimated effects with their standard error was considered. If the estimated effect is larger than the standard error, that effect is considered significant. The estimate of effects and their standard error were obtained

from Eqs.3.3 and 3.4. The calculation of estimated effects and standard error of estimated effect are shown in Appendix B. The results from this study are as follows:

4.3.1 Stress-Strain Curves of Eight Experiments in Experimental Design

Figure 4.4 shows stress-strain curves of the eight (2^3) experiments in factorial design. All curves are those exhibited by elastomeric materials. See raw data in Appendix C (Table C-6).
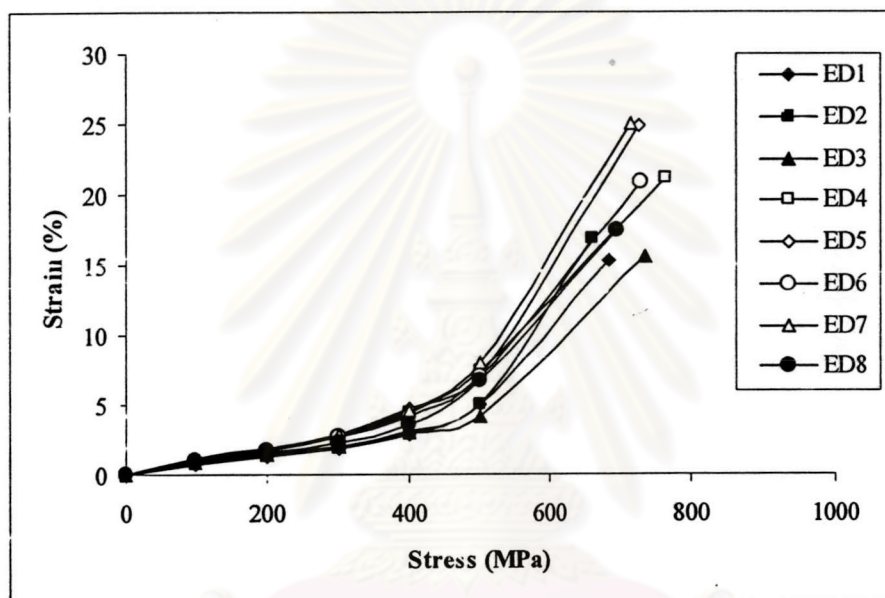

Figure 4.4 Stress-strain curves of 8 (2^3) experiments in '2^k experimental design'

(Keys for sample labels are listed in Table 4.3)

4.3.2 Effects on Tensile Modulus at 300% Elongation (M300)

The estimated effects of the factorial analysis on tensile modulus along with the standard error of the effects are given in Table 4.4.

Table 4.4 The estimated effects on tensile moduls at 300% elongation (M300)

Effect	Estimated effect	Standard error
Main effect		
TEOS (T)	0.681	± 0.044
NH$_3$ (N)	0.212	± 0.044
Gelation time (G)	0.221	± 0.044
Two factor interaction		
TN	-0.083	± 0.044
TG	0.003	± 0.044
NG	0.054	± 0.044
Three factor interaction		
TNG	-0.017	± 0.044

It was found that factors that influence M300 are T, N, G, TN and NG. Nevertheless, the estimated effects value of NG is close to the standard error, indicating that NG is not highly significant effects for the M300 of these composites.

The three main effects are plotted against M300 (Fig. 4.5). It can be seen that increasing T, N, and G result in an increase of M300. The composite with all three effects at a high level is used to maximize the tensile modulus. However, the N effect is less important than the others [Fig.4.5 (c)]. Note from the TN interaction effect [Fig. 4.5(d)] that additional ammonia does not significantly effect the tensile modulus when TEOS content is high. Therefore, a composite with large M300 value can be obtained by adding large amount of TEOS but limit the ammonia content to a low amount. For practical usage, a high M300 value requires high TEOS content, long gelation time, and no need to add more NH$_3$ into the latex.
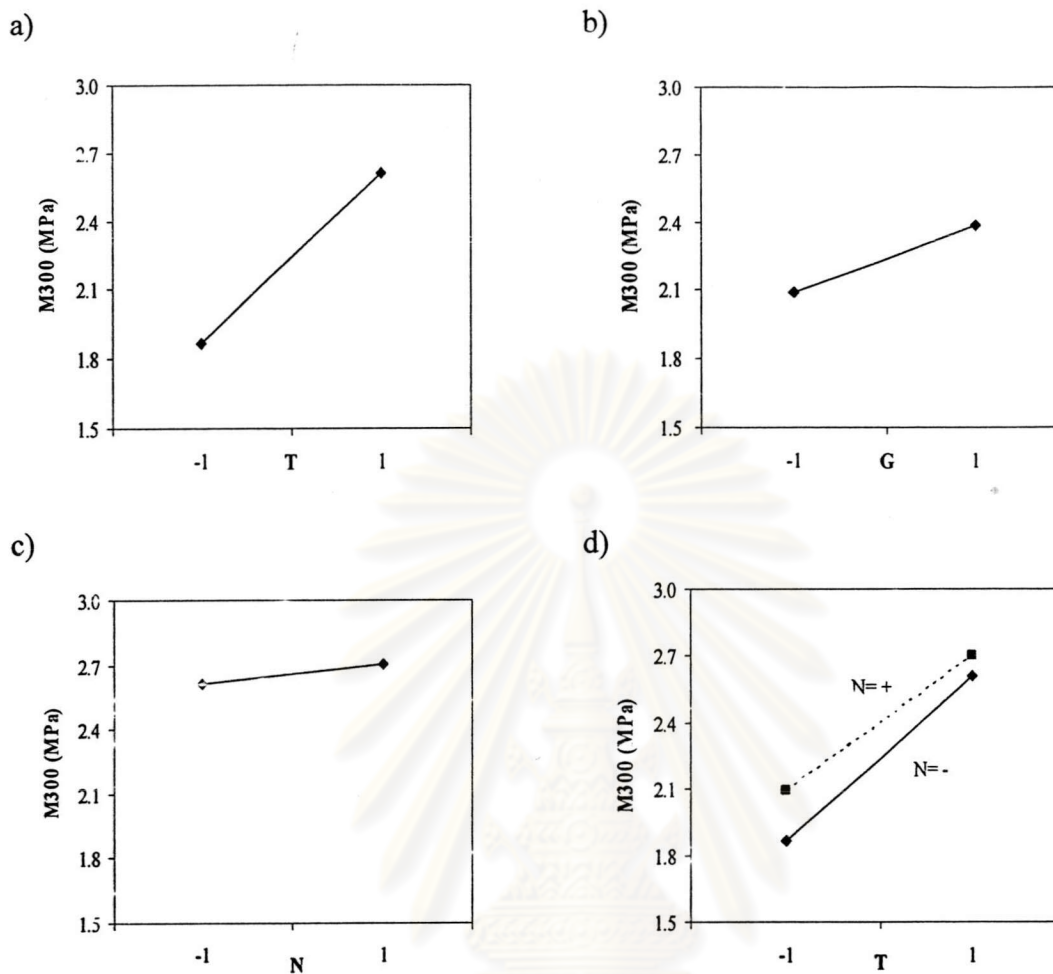
Figure 4.5 The effect of (a) T, (b) G, (c) N and (d) TN interaction on M300

4.3.3 Effects on Tensile Strength

The estimated effects of the factorial analysis on tensile strength are given in Table 4.5 along with the standard error of the effects. It is found that factors that influence tensile strength of the composites are T, G and TN.

Table 4.5 The estimated effects on tensile strength of the NR composites

Effect	Estimated effect	Standard error
Main effect		
TEOS (T)	6.61	± 0.96
NH_3 (N)	0.83	± 0.96
Gelation time (G)	1.34	± 0.96
Two factor interaction		
TN	-1.41	± 0.96
TG	0.65	± 0.96
NG	0.59	± 0.96
Three factor interaction		
TNG	0.25	± 0.96

The results of main effect T and G shown in Fig 4.6(a) and (b), indicating that increasing T and G or high TEOS content and long gelation time will result in an increase of tensile strength. The TN interaction effect is plotted in Fig. 4.6(c). From the plot, when using high TEOS content, increasing ammonia becomes less effective in increasing the tensile strength. Therefore, a composite with highest tensile strength can be obtained by adding large amount of TEOS but limit the ammonia content to a low amount. In another word, there is no need to add more ammonia to the concentrated NR latex that already contains 0.7% NH_3.
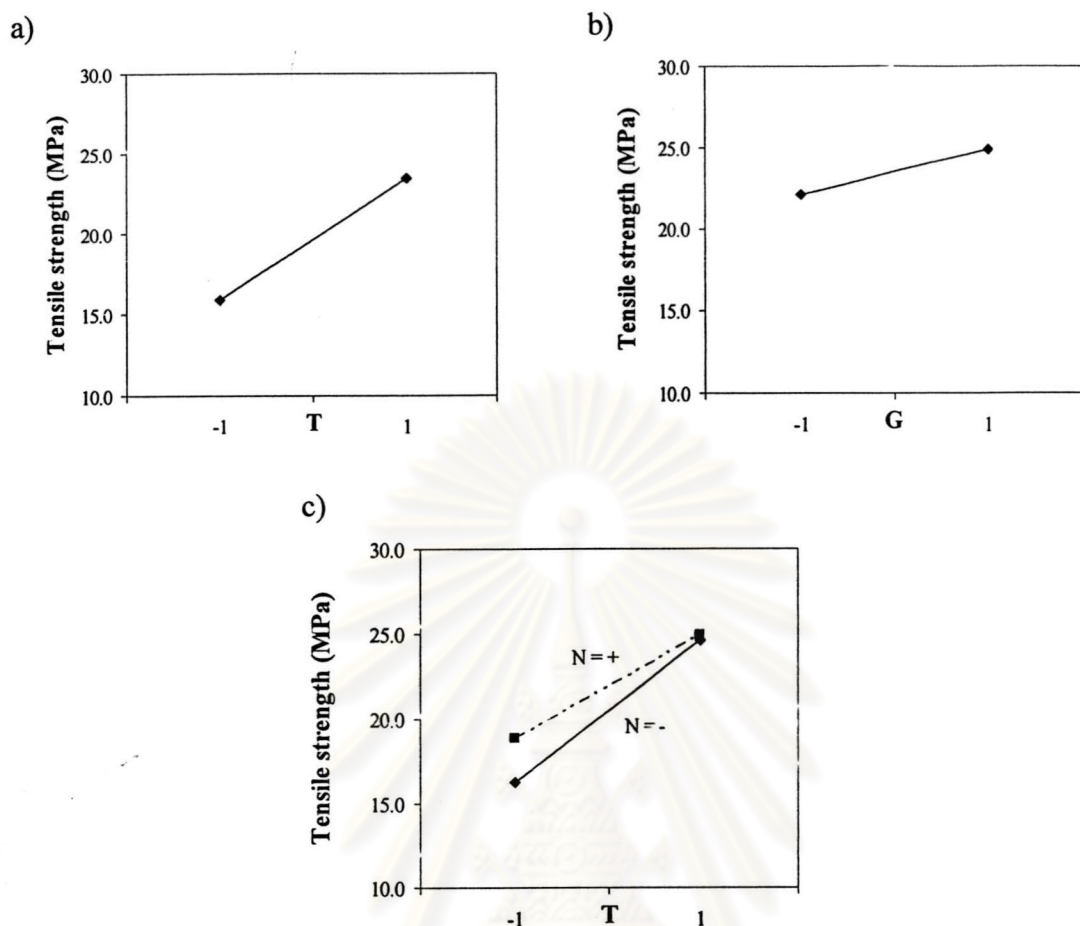
a)

b)

c)

Figure 4.6 The effect of (a) T, (b) G and (c) TN interaction on tensile strength

4.3.4   Effects on Tear Strength

The estimated effects of the factorial analysis on tear strength are given in Table 4.6 along with the standard error of the effects. Factors that influence tear strength of the composites are T, G, TG and TNG. Nevertheless, the estimated effects value of TG is close to standard error, suggesting that TG interaction effect does not significantly affect the tear strength of these composites.

For the main effects- T and G (Fig. 4.7), increasing either factor will result in an increase of tear strength. It is also found that the three-interaction effect (TNG), however, gives a minus sign. This indicates that increasing the amount of one factor can cause a reduction of tear strength. From Table 4.3, the highest tear strength was obtained from sample ED7 (T+, N-, G+). This implies that ammonia is the one that should be limited to a low value. Nevertheless, results from Table 4.6 suggest that NH_3

does not have a significant effect on tear strength when compare to other main effects. For practical usage, the highest tear strength would require high TEOS content (50 phr), long gelation time (10 days), and no need to add more NH_3 into the latex.

Table 4.6 The estimated effects on tear strength

Effect	Estimated effect	Standard error
Main effect		
TEOS (T)	5.13	± 0.68
NH_3 (N)	-0.17	± 0.68
Gelation time (G)	1.17	± 0.68
Two factor interaction		
TN	-0.63	± 0.68
TG	1.00	± 0.68
NG	-0.45	± 0.68
Three factor interaction		
TNG	-1.89	± 0.68

a)   b)
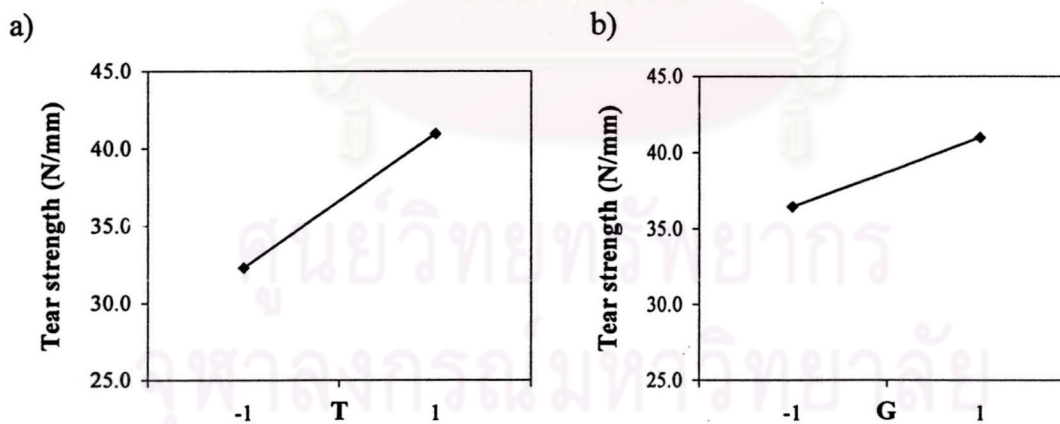
Figure 4.7 The effect of (a) T and (b) G on tear strength

4.4 Comparison Between *in situ* Silica and Mechanically Mixed Silica

In this section, curing time, Mooney viscosity, tensile modulus, tensile strength, and tear strength of the composite containing *in situ* silica were analyzed. The data were then compared to the composite that was mechanically filled with the same amount of silica. The silica powder used here was an industrial grade that was used regularly in composite industries. Comparison between the *in situ* silica and mechanically mixed silica was made as follows.

4.4.1 Stress-Strain Curve

The stress-strain curves of NR-silica composites listed in Table 4.2 are shown in Fig. 4.8. All curves are those exhibited by elastomeric materials. Discussions on tensile modulus and strength of the composite filled with *in situ* silica and mechanically-mixed silica are in the following section. See raw data in Appendix C (Table C-7).
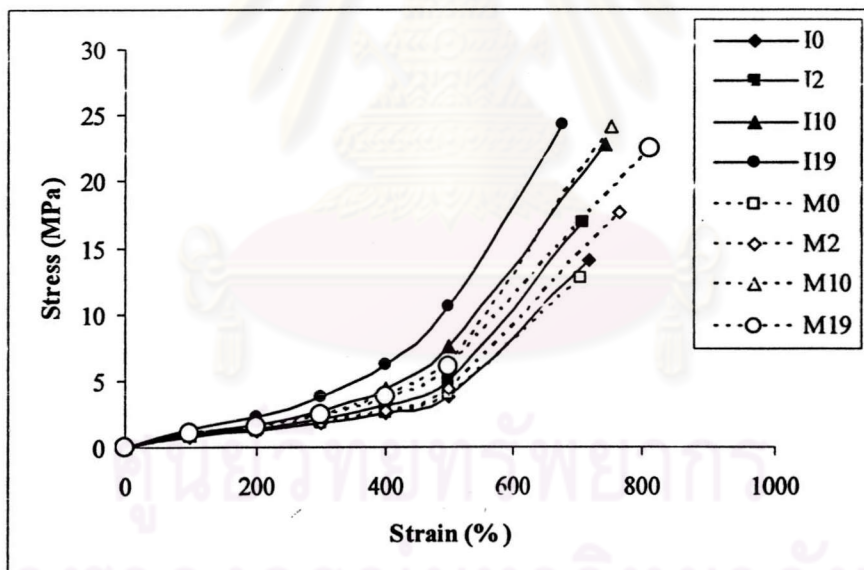

Figure 4.8 Stress-strain of NR-silica composite having various silica contents

('Ix' and 'Mx' denote composites filled with n% *in situ* silica and n% mechanically-mixed silica respectively.)
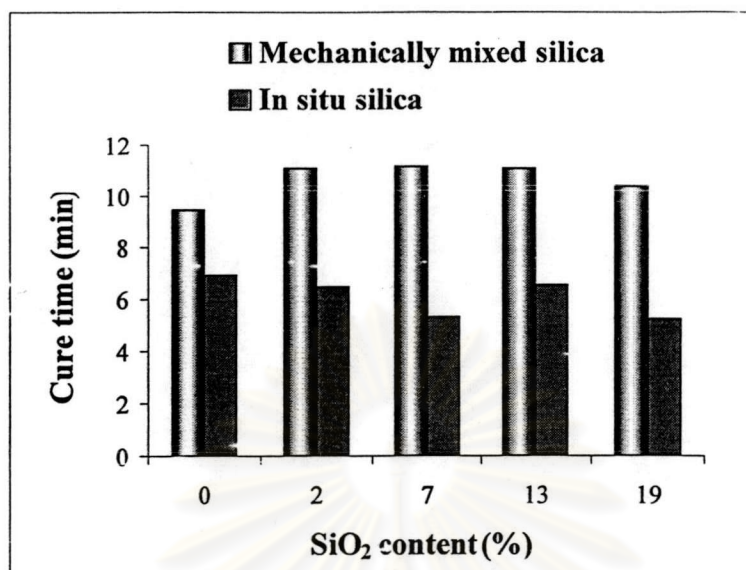
4.4.2 Cure Time

Figure 4.9 Cure time (t_{90}) of NR-silica composite having various silica contents

A plot of cure time or t_{90} versus the amount of silica in the composites was shown in Fig. 4.9. The t_{90} of the composite containing mechanically mixed silica is higher than the one with *in situ* silica. This means that the composite filled with mechanically mixed silica needs a longer time to complete curing process than the one with *in situ* silica. See all data in Appendix C (Table C-1).

4.4.3 Mooney Viscosity

In general the Mooney viscosity (ML1+4 @100°C) of the composites increased as expected when increasing silica contents (Fig. 4.10). The viscosity of the composite with conventionally mixed silica powder is higher than the one with *in situ* silica. According to Ikeda [13], the silica powder in the rubber matrix can aggregate and forms pseudo-network structure. This leads to a significant increase of viscosity. Here, the viscosity results suggest that the degree of aggregation of the composite having *in situ* silica is less than the one with conventionally mixed silica. It is possible that the interaction among the *in situ* silica particles is smaller than that among the conventionally mixed silica powder. See all data in Appendix C. (Table C-2).
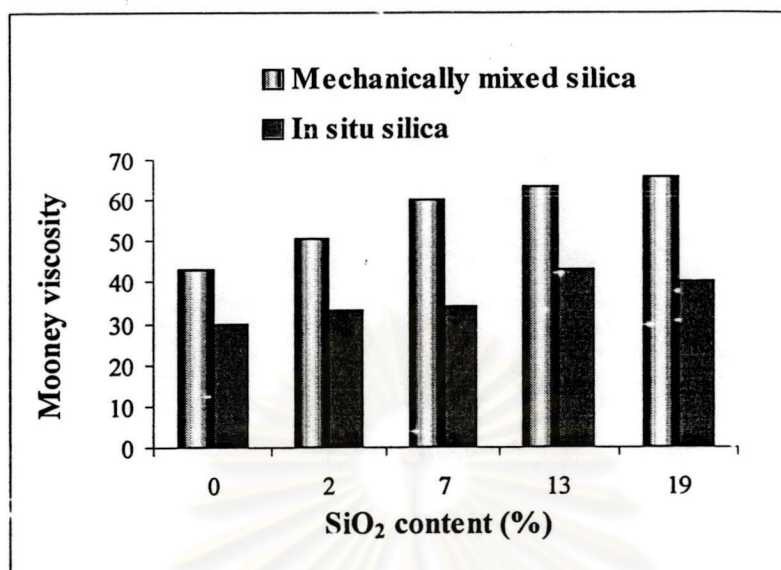
Figure 4.10 Mooney viscosity of NR-silica composite having various silica contents

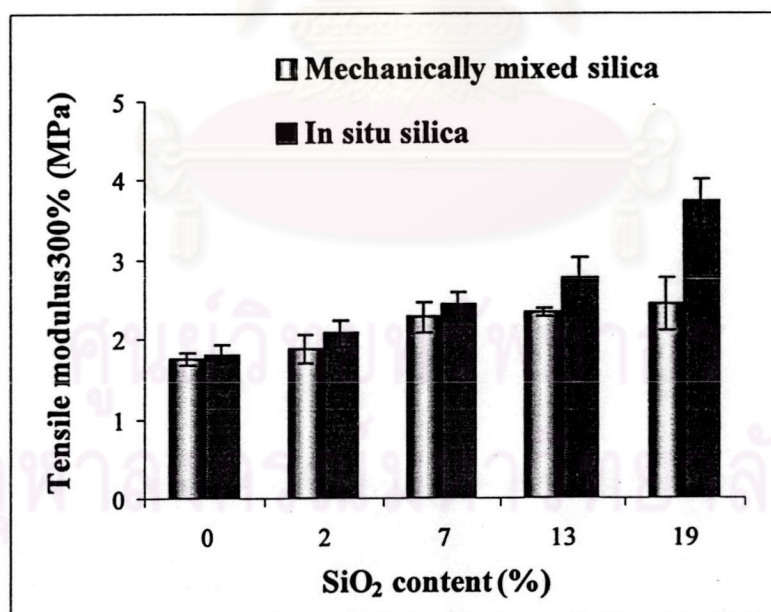### 4.4.4 Tensile Modulus at 300% Elongation (M300)

Figure 4.11 Tensile modulus at 300 % elongation of vulcanized NR-silica composite having various silica contents

The bar-graph in Fig. 4.11 exhibits the effect of silica loading on tensile modulus. The modulus of the composite containing *in situ* silica is slightly higher than the one with mechanically mixed silica (see all data in Appendix C). The difference becomes more distinct at high silica content.

4.4.5 Tensile Strength

From Fig. 4.12, it is clear that the tensile strength of the composites increases with increasing silica contents. However, the tensile strength values of the composite filled with two types of silica are not significantly different from one another in the samples being studied (see all data in Appendix C).
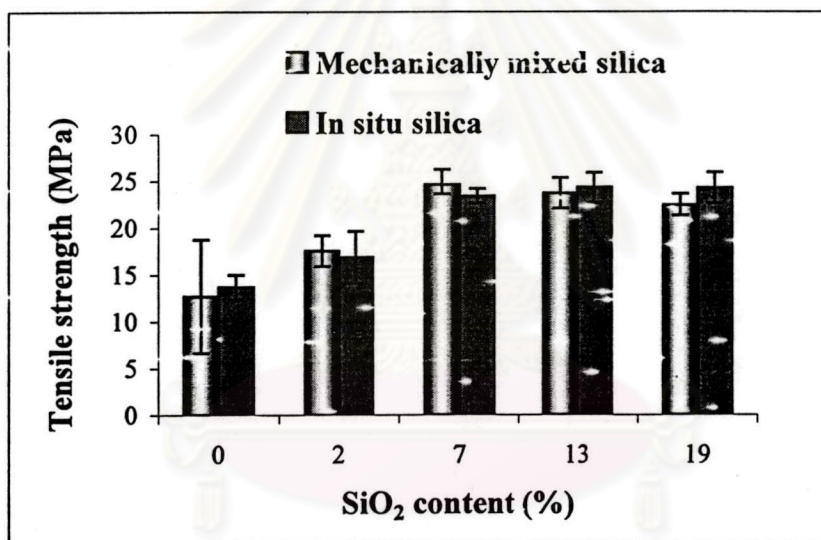

Figure 4.12 Tensile strength of vulcanized NR-silica composite having various silica contents

4.4.6 Tear Strength

Tear strength of the composite of *in situ* silica is higher than that of the mechanically mixed silica (Fig. 4.13). At higher silica content, the tear strength is obviously more different (see all data in Appendix C).
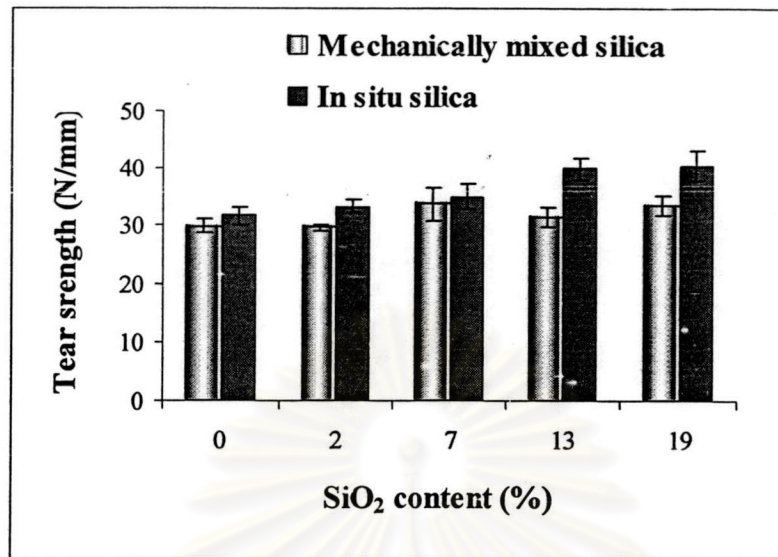
Figure 4.13 Tear strength of vulcanized NR-silica composite having various silica contents

These results suggest that silica that was generated *in situ* has a better reinforcement efficiency than silica powder. This could be due to a better interface between silica and NR chain in the case of silica formed *in situ*.